

Review

# MHD Accretion Disk Winds: The Key to AGN Phenomenology?

Demosthenes Kazanas 

NASA/Goddard Space Flight Center, 8800 Greenbelt Rd, Greenbelt, MD 20771, USA; demos.kazanas@nasa.gov;  
Tel.: +1-301-286-7680

Received: 8 November 2018; Accepted: 4 January 2019; Published: 10 January 2019

**Abstract:** Accretion disks are the structures which mediate the conversion of the kinetic energy of plasma accreting onto a compact object (assumed here to be a black hole) into the observed radiation, in the process of removing the plasma's angular momentum so that it can accrete onto the black hole. There has been mounting evidence that these structures are accompanied by winds whose extent spans a large number of decades in radius. Most importantly, it was found that in order to satisfy the winds' observational constraints, their mass flux must increase with the distance from the accreting object; therefore, the mass accretion rate on the disk must decrease with the distance from the gravitating object, with most mass available for accretion expelled before reaching the gravitating object's vicinity. This reduction in mass flux with radius leads to accretion disk properties that can account naturally for the AGN relative luminosities of their Optical-UV and X-ray components in terms of a single parameter, the dimensionless mass accretion rate. Because this critical parameter is the dimensionless mass accretion rate, it is argued that these models are applicable to accreting black holes across the mass scale, from galactic to extragalactic.

**Keywords:** accretion disks; MHD winds; accreting black holes

---

## 1. Introduction-Accretion Disk Phenomenology

Accretion disks are the generic structures associated with compact objects (considered to be black holes in this note) powered by matter accretion onto them. Their formation is a consequence of the fact that the specific angular momentum of the accreting matter at the outer boundary of the flow is larger than its Keplerian value on the accreting body vicinity. The role of the accretion disk is to rid this excess angular momentum of the disk plasma and allow it to accrete onto the gravitating compact object. This process is effected by viscous stresses which at the same time cause the heating of the accreting matter and emission of radiation with rather specific spectral characteristics.

The present article is not a review of accretion disks (the interested reader can consult several such reviews e.g., [1]); instead, it aims to present alternatives to the more conventional accretion disk views which are driven by accumulating phenomenology of the spectroscopic properties of the winds that are ubiquitous in accretion powered compact objects. The hope is that these alternative views will lead to novel, fruitful insights on the structure of these systems. As such, this note focuses on only certain specific issues while ignoring many others along with some of the important works on the subject. Because it argues for the scale invariance of the accretion disk winds, it includes in the discussion properties of winds and accretion disks onto black holes of both Galactic X-ray binaries (XRB) and active galactic nuclei (AGN) to support the mass invariance by as large of mass range as possible. At the end, it is argued that, in their broader sense, the global spectral properties of accreting black holes can be accounted for in terms of a small number of parameters, if one is willing to accept certain facts associated with the general properties of their observed outflows obtained through X-ray spectroscopy.

Much of the work on accretion powered sources has been based on and influenced by the seminal work on the subject, namely that of Shakura and Sunyaev (hereafter SS73) [2]. This work assumes the disks to be steady-state, roughly Keplerian ( $v_r \ll v_\phi$ ), thin ( $h \ll R$ ) and in hydrostatic equilibrium in the vertical direction. The disk temperature is obtained by solving their thermal balance (local energy dissipation equals the energy radiated; see Section 2.1). The dissipation is effected by the viscous stresses, assumed to be proportional to the local gas pressure  $P$  ( $t_{r\phi} \simeq \alpha P$ );  $\alpha \sim 0.1$  is an unknown parameter to be determined by observation or simulation. The same viscous stresses serve also to transfer outward the excess angular momentum of the disk plasma, allowing its further accretion.

The usual assumption in most treatments is that all energy involved in the transfer of angular momentum is dissipated locally. However, one should note that since angular momentum cannot be destroyed and since essentially all the disk kinetic energy is stored in its angular motion, none of that energy could be dissipated. However, viscous stresses can dissipate circulation and presumably it is the dissipation of circulation that powers the observed radiation of accretion disks. Because in axisymmetry circulation has the same form as the non-dissipative angular momentum, one can speculate that the observed presence of dissipation in accreting objects involves non-axisymmetric fluid modes.

A further simplifying assumption generally made in modeling accretion disks is that the dissipated energy is thermalized, i.e., that the disk particles achieve a thermal distribution of temperature determined by energy balance, with the emitted radiation being of black body form. This then can determine the disk temperature radial profile: In steady-state disks (mass flux  $\dot{M}$  independent of time and radius) the local energy dissipation per unit area is proportional to  $3GM\dot{M}/8R^3$ ; setting equal to  $\sigma T^4$  (black body emission), implies a disk temperature dependence  $T \propto R^{-3/4}$ , with a multi-color flux density  $F_\nu \propto \nu^{1/3}$  photons  $\text{cm}^{-2} \text{s}^{-1}$  ( $R$  denotes the cylindrical radial coordinate along the disk equatorial plane and  $r$  the spherical coordinate).

The innermost disk temperature can be estimated assuming that the emitting surface is roughly  $\pi r_{ISCO}^2$  (ISCO is short for the innermost stable circular orbit; for a Schwarzschild black hole  $r_{ISCO} \simeq 3R_S \simeq 10^6 M_0 \text{ cm}$ , where  $R_S = 2GM/c^2$  is the Schwarzschild radius and  $M_n = M/10^n M_\odot$  is the black hole mass in  $10^n$  solar masses). An estimate of the disk highest temperature, then, requires a value of the disk luminosity. Because the maximum luminosity of an accretion powered source is generally considered to be the object's Eddington luminosity,  $L_{\text{Edd}} \simeq 1.3 \times 10^{38} M_0 \text{ erg/s}$ , the corresponding maximum disk temperature is  $T \simeq 10^{7.5} M_0^{-1/4} \text{ K} = 10^{5.5} M_8^{-1/4} \text{ K}$ . The fact that quasi-thermal, multi-color features at the corresponding temperatures were observed at approximately these energies in galactic XRBs and AGNs have established the SS73 disk as a ubiquitous structure in both these classes of sources.

However, besides these quasi-thermal, multi-color spectral components it was established, that a large fraction of these objects' luminosity is shared by a spectral component of power-law form that extends to energies  $E \simeq 100 \text{ keV}$ , clearly inconsistent with that of thermal radiation by an accretion disk. In analogy with the Sun, this component was then attributed to the presence of a hot ( $T \sim 10^8\text{--}10^9 \text{ K}$ ) corona, overlaying the accretion disk [3]. Again, in analogy with the solar corona, this was proposed to be powered by magnetic fields that thread the accretion disk and dissipate part of its energy in this hot corona, which then Compton-scatters the disk thermal radiation to produce the observed high energy photons.

The advent of observations and data accumulation, then, established that the ratio of luminosities of these major accretion disk spectral components is not random but varies in a systematic way, generally with the contribution of the quasi-thermal disk component increasing with the objects' bolometric luminosity (a proxy for the accretion rate  $\dot{M}$ ) and that of the harder, power-law one waning. Thus, for AGN (where the multi-color component referred to as the Big Blue Bump (BBB) is in the UV/Optical band, well separated from the power-law X-ra component) it was found that the logarithmic flux slope between the UV (2500 Å) and 2 keV X-ray fluxes, the so-called  $\alpha_{\text{OX}}$  parameter, increases (in absolute value; it becomes more negative) with increasing source luminosity [4].

A similar correlation appears to be present in XRBs between their multi-color disk component and their power-law X-rays (see [5] for a review). The reason for the observed correlation (Figure 4 of [4]), is not clear (we will present an account in Section 4). Another open issue is the geometry of the X-ray emitting plasma relative to the BBB component. Earlier models based on emission by a magnetically powered corona, assumed that the X-ray emitting plasma was overlying the BBB emitting thin accretion disk. However, issues concerning the cooling of the corona electrons [6], and the corresponding variability due to reprocessing of the X-rays on the thin disk [7], appear to require refinement of this geometric arrangement.

Accretion disk theory got a big boost in the 90's with two significant developments: (i.) Balbus and Hawley [8] showed that a fluid rotating with angular velocity  $\Omega$  and threaded by poloidal magnetic field is stable if  $d\Omega^2/dr > 0$  (in disagreement with Rayleigh criterion for unmagnetized flows that demands  $d(\Omega^2 r^4)/dr > 0$ ). According to this criterion, Keplerian accretion disks are unstable, with the magnetic field acting as the agent that helps mediate the transfer of angular momentum necessary for accretion to take place (for a pedagogical discussion of this instability and why it does not reduce to the Rayleigh criterion as the magnetic field goes to zero see [9,10]). (ii.) Narayan and Yi [11,12] produced models of accretion disks that are optically thin and geometrically thick ( $h \simeq R$ ), supported at each radius by the pressure of ions, referred to as Advection-Dominated Accretion Flows (ADAF). The rotational velocity of these disks is sub-Keplerian with  $v_r \simeq v_\phi \lesssim v_K$ .

The reason the ADAF disks are thick is that the proton cooling time (assuming they achieve at some radius  $r$  their virial temperature, i.e.,  $kT_p \simeq GMm_p/r$ , heated both by the dissipation of the azimuthal motions and the  $pdV$  work of accretion) through Coulomb collisions with the cooler electrons, is longer than the local viscous time scale, which for  $h \simeq R$  is only  $\alpha$  times longer than the free fall time  $t_{ff} \simeq R/v_r$ . Such thick flows, are therefore possible only for  $t_{cool} > t_{visc}$ . As shown in Section 2.2, the condition  $t_{cool} > t_{visc}$  reduces to a condition involving just the normalized accretion rate (see Section 2)  $\dot{m} < \alpha^2$ . It is interesting that this condition involves neither the mass of the object  $M$  nor the radius of the flow  $x$  (see however [12] for a weak  $x$ -dependence), implying that such flows are self-similar and scale free if expressed in normalized parameters. Flows with  $\dot{m} < \alpha^2$ , if they start hot (i.e., with virialized protons), they will remain so all the way to the horizon of the accreting body with their azimuthal and radial velocities a fraction of the Keplerian one ( $v_\phi \simeq v_r \sim 0.7v_K$ ). Because their disk height  $h \simeq R$ , they resemble spherical accretion; also, because their cooling time is longer than the advection time onto the accreting object, their radiative efficiency is reduced by a factor  $t_{visc}/t_{cool} \sim \dot{m}$  and the accretion luminosity  $L$  is no longer simply proportional to  $\dot{m}$  but to  $\dot{m}^2$ . As such they are referred to as either ADAF or RIAF (Radiatively Inefficient Accretion Flows).

The great advantage offered by the ADAF paradigm is that it provides the hot electrons demanded by the hard X-ray observations of (galactic and extragalactic) black holes as a result of the general accretion flow dynamics, rather than as a corona, unrestricted by the dynamics of accretion and introduced so that it would accommodate the observations. The notion of ADAF, then, led to a hybrid picture for the spectral decomposition of galactic binary X-ray sources [13] (see Section 2.2).

Besides the above features, ADAF have an additional distinct property: Their Bernoulli integral,  $Be$ , the sum of their kinetic, thermal and potential energies per unit mass is positive, a fact noted in the original references on the subject [11,12]; therefore, these flows provide for the potential presence of outflows that are apparently ubiquitous in accretion powered sources [14] (this is not the case in SS73 disks whose internal thermal energy is radiated promptly away resulting in  $Be < 0$ ). The reason for the positivity of  $Be$  was elucidated in a (very important in this author's opinion) paper by Blandford and Begelman [15]: The viscous stresses that transfer outward the fluid's angular momentum, so that it is allowed to sink deeper into the gravitational potential, transfer also mechanical energy (see Section 2.1); while in an SS73 disk this energy is radiated away on time scales shorter than its viscous time scale, in an ADAF it remains stored in the fluid for longer time, that being reason behind the positivity of  $Be$ .

The solution of the conundrum, offered in [15], is that the excess energy and angular momentum are expelled off the disk in the form of a wind providing thus a combination of advection-dominated

inflow - outflow solutions (ADIOS). This leaves the disk with less matter to accrete but with matter that it is now bound gravitationally, i.e., with  $Be < 0$ . As a result, the accretion rate  $\dot{m}$  is no longer constant but depends on the (normalized) radius  $x = r/R_S$ , i.e.,  $\dot{m} = \dot{m}(x)$  ( $R_S$  is the black hole Schwarzschild radius). The authors of [15] did provide simple models of radius dependent winds with mass flux of the form  $\dot{m}(x) \propto x^p$  and  $1 > p > 0$ . The positive value of  $p$  implies that these flows eject a wind most of the mass available for accretion at their outer edge, thereby the name ADIOS.

The structure of this article is as follows: In Section 2 we give a brief review of the structure of accretion disks and the modifications and effects introduced by the notion of ADAF and ADIOS. In Section 3 we outline the X-ray spectroscopic observations and indicate that they support winds and accretion disks of the form of ADIOS; we present and discuss the results of photoionization calculations of ADIOS-like MHD winds, to show they are consistent with the X-ray absorber observations. In Section 4 we indicate how these winds can reproduce the trend in  $\alpha_{OX}$  on luminosity in AGN and conclude in Section 5 with a brief summary of these results and conclusions.

## 2. The Physics of Accretion Disks

### 2.1. The Structure of Accretion Disks

The structure of accretion disks is given by the transfer of angular momentum, hydrostatic equilibrium in the direction perpendicular to the disk plane and the mass and energy flux conservations. Finally, the disk spectrum is computed assuming that all energy released locally is dissipated and emitted in black body form.

*i. Hydrostatic equilibrium:* This assumption of a thin disk implies

$$\frac{dP}{dz} = -\rho \frac{GM}{r^2} \frac{z}{r} \quad \text{or} \quad \frac{P}{h} \simeq \rho \frac{GM}{r^2} \frac{h}{r} \quad (1)$$

upon setting  $\Delta P \approx P$  and  $\Delta z \approx h \approx z$

$$\frac{P}{\rho} \simeq c_s^2 \simeq \frac{GM}{r} \frac{h^2}{r^2} = V_K^2 \frac{h^2}{r^2} \simeq \Omega^2 h^2 \quad (2)$$

where  $\Omega, V_K$  are the disk Keplerian frequency and velocity; then the disk height read  $h \simeq c_s/\Omega$ , where  $c_s \simeq (P/\rho)^{1/2}$  is the sound speed in the disk.

*ii. Angular Momentum Conservation:* If  $\dot{J} = \dot{M}(GM/r)^{1/2}$  is the rate at which angular momentum is transported inward at radius  $r$  by the accretion of matter at accretion rate  $\dot{M}$ , and  $\dot{J}_I = \dot{M}(GM/r_I)^{1/2}$  the rate at which angular momentum accreted onto the black hole at its innermost, stable, circular orbit radius (ISCO)  $r_I = 3R_S$  ( $R_S$  is the black hole Schwarzschild radius), their difference implies the presence of a torque  $\mathcal{T} = t_{r\phi}(2h \cdot 2\pi r) \times r = \dot{J} - \dot{J}_I$ , which transfers their difference outward. In this expression  $t_{r\phi}$  is the viscous stress (i.e., the force per unit area in the  $\phi$ -direction) and  $2h$  the total thickness of the disk. It is generally assumed [2] that the viscous stress is proportional to the local pressure  $P$ , so that  $t_{r\phi} = \alpha P$  with  $\alpha < 1$ .

Angular momentum conservation then leads to the expression for the stress  $t_{r\phi}$

$$2ht_{r\phi} = \frac{\dot{M}}{2\pi r^2} (GM/r)^{1/2} \left[ 1 - \zeta \left( \frac{r_I}{r} \right)^{1/2} \right] = \frac{\dot{M}}{2\pi r^2} (GM/r)^{1/2} J(r) \quad (3)$$

The term in square brackets indicates the fact that matter freely falls onto the black hole for radii  $r < r_I$  with  $\zeta = 1$  if the torques are also zero at the same point.

With the above expression for the stresses, one can then compute the heat generation rate per disk unit area,  $2Q$  ( $Q$  is the emission from each side of the disk), considering that the energy so

generated *per unit volume* is  $\dot{\epsilon} = 2t_{r\phi}\sigma_{r\phi}$ , on substituting  $2ht_{r\phi}$  from Equation (3) above, with  $\sigma_{r\phi} = (3/4)\Omega = (3/4)(GM/r^3)^{1/2}$ . So,

$$2h\dot{\epsilon} = (2ht_{r\phi})(2\sigma_{r\phi}) = 2Q = \frac{3\dot{M}}{4\pi r^2} \frac{GM}{r} J(r) \quad (4)$$

Therefore, the heat generated from a radius  $r_1 (\gg r_I)$  to infinity is

$$2Q_{tot}(r_1) = \int_{r_1}^{\infty} 2h\dot{\epsilon} 2\pi r dr \simeq \frac{3}{2}\dot{M} \frac{GM}{r_1} \quad (5)$$

One should note that gravitational energy  $V$  from infinity to  $r_1$  is released at a rate  $G\dot{M}M/r_1$ , but because of the virial theorem,  $2T + V = 0$ , only half of this can be converted to heat, with the rest remaining as orbital energy ( $T = V/2$ ). Thus, the rate at which gravitational energy is converted into heat is  $G\dot{M}M/2r_1$ .

The difference between the above expression and that of Equation (5) is provided by the viscous stresses which transport outward not only angular momentum but also energy at a rate [16]

$$\dot{E} = \Omega\mathcal{T} = \Omega 2\pi r^2 2ht_{r\phi} = \frac{G\dot{M}M}{r_1} J(r_1) \simeq \frac{G\dot{M}M}{r_1} \quad (r \gg r_I) \quad (6)$$

As noted in [15], this is an important issue because in cases that the energy transferred by viscous stresses cannot be radiated away on a viscous time scale (e.g., ADAF), it leads to positive Bernoulli integral. Flows in 2D (i.e.,  $r, \phi$ ) with  $Be > 0$  would not be then possible to accrete. To remedy this situation, [15] proposed that the excess energy and angular momentum escape in the  $\theta$ -direction in the form of a wind, thereby allowing matter in the disk to flow to the compact object. Because the disk span a large number of decades, the authors of [15] provided simple wind models with wind mass flux  $\dot{M}_w$  depending on the radius e.g.,  $\dot{M} = \dot{M}(r) \propto r^p$ ,  $0 < p < 1$ , i.e., with mass flux increasing with radius; this should not be surprising, considering that so does the disk specific angular momentum. Therefore, as matter accretes through the disk, it also "peels-off" in a wind away from the disk plane, carrying away the excess disk angular momentum and torque - transferred energy from its inner sections, setting the disk  $Be$  to a negative value, while at the same time reducing the mass flux remaining in the disk to be accreted onto the compact object (the notion of a decreasing mass flux in the disk goes against the overwhelming majority of works on the subject). The outward increasing mass flux of these winds has significant observational consequences that appear consistent with observations [17,18]. We propose that this last fact is responsible for much of the AGN and XRB phenomenology, as it will be discussed below.

## 2.2. General Accretion Disk Scalings

It is instructive to present the accretion disk equations in dimensionless form, as this makes apparent the dependence of their properties relative to their natural units, most notably their accretion rate in terms of the Eddington accretion rate and the Schwarzschild radius. Normalizing the disk radius  $r$  by  $R_S$ , i.e., setting  $r = x R_S$ , and its accretion rate by the Eddington accretion rate, i.e., setting  $\dot{M} = \dot{m} \times \dot{M}_{Edd}$ , with  $\dot{M}_{Edd} = L_{Edd}/c^2 = 2\pi m_p c R_S / \sigma_T \propto M$ , the hydrostatic equilibrium and angular momentum transfer equations (Equations (2) and (3)) can be both solved for the disk pressure  $P$  to obtain (bearing in mind the prescription  $t_{r\phi} = \alpha P$ )

$$P = \rho \frac{GM}{r^2} \frac{h^2}{r} = \frac{m_p c^2}{2} n(x) x^{-1} \left(\frac{h}{r}\right)^2 \quad (7)$$

$$P = \frac{\dot{M}}{4\pi\theta\alpha} \frac{(GMr)^{1/2}}{r^2} J(r) = \frac{m_p c^2}{\sigma_T R_S} \dot{m}(x) x^{-5/2} \left(\frac{h}{r}\right)^{-1} \frac{J(x)}{2\sqrt{2}\alpha} \quad (8)$$

with  $J(x) = 1 - (3/x)^{1/2}$ , and following the arguments given in the introduction we assume that the accretion rate  $\dot{m}$  is also a function of the radius  $x$ .

From the above equations one can obtain an expression for the disk density  $n(x)$

$$n(x) = \frac{\dot{m}(x)}{\sigma_T R_S} x^{-3/2} \left(\frac{r}{h}\right)^3 \frac{J(x)}{2^{1/2} \alpha} \quad (9)$$

and for the energy emitted per unit disk area (from one of its sides)

$$Q = \frac{3}{8\pi} \frac{GM\dot{M}(r)}{r^3} J(r) = \frac{3}{4} \frac{m_p c^3}{\sigma_T R_S} x^{-3} \dot{m}(x) J(x) \quad (10)$$

The total luminosity can be obtained by integrating the above expression over the surface of the disk  $2\pi r dr$  from  $r_I$  to infinity, i.e., (one must use  $2Q$  to take into account both sides of the disk)

$$L = \int_{r_I}^{\infty} (2Q) 2\pi r dr = \frac{GM\dot{M}}{r_I} \left(\frac{3}{2} - \zeta\right) = \frac{\pi m_p c^3}{\sigma_T} \frac{R_S \dot{m}(x)}{x_I} \left(\frac{3}{2} - \zeta\right) \quad (11)$$

It is generally assumed that the pressure  $P$  is given either by the sum of gas and radiation pressures, each becoming dominant at different radii of the disk and for different values of the accretion rate  $\dot{m}(x)$ . Each such approximation leads to different run of the disk parameters with the radius  $x$  (see [19] for a detailed study). At present we will include also magnetic pressure. For simplicity, herein we will assume only gas and magnetic pressures  $P_g, P_B$ , with the magnetic pressure being dominant (see also [20]) and the stresses being again proportional to  $\alpha(P_g + P_B)$ . The presence of three components of the magnetic stresses makes the problem necessarily more complicated; however, we will consider here only their contribution to the vertical disk structure. The inclusion of magnetic field contribution in the disk vertical structure divorces the disk height from the local plasma temperature, thereby allowing transitions between hot and cool states as implied by observations and detailed in the next subsection.

Even at this simplified approach, the system likely entails far more detail than presented herein (e.g., field annihilation on an equatorial current sheet). Our simplified model averages all that over the disk height. Then the total pressure, in conjunction with the hydrostatic equilibrium expression, reads

$$P = \frac{B_\phi^2(x)}{4\pi} + n(x) m_p c_s^2 = \rho(x) \frac{GM}{r^3} h(x)^2 \quad (12)$$

where  $c_s(x)$  is the sound speed of the gas. Considering that  $B_\phi^2/4\pi\rho(x) = V_A^2$  with  $V_A$  the Alfvén velocity, and that  $GM/r = V_K^2$ , the disk Keplerian velocity, the hydrostatic equilibrium condition reads

$$\frac{h^2}{r^2} = \frac{B_\phi^2}{4\pi\rho V_K^2} [1 + \beta(x)] = \frac{V_A^2}{V_K^2} [1 + \beta(x)] \quad (13)$$

where  $\beta(x)$  is the usual gas-to-magnetic pressures parameter of the plasma.

From mass conservation (bearing in mind that, as discussed above the accretion rate depends on the radius  $r$ ),

$$\dot{M}(x) = 2\pi h r n(x) m_p V_r \quad (14)$$

and employing Equation (9), we obtain an expression for the radial flow velocity  $V_r$

$$\frac{V_r}{c} = \frac{1}{x^{1/2}} \left(\frac{h}{r}\right)^2 \frac{\alpha}{J(x)} \quad \text{or} \quad \frac{V_r}{V_K} \simeq \left(\frac{h}{r}\right)^2 \frac{\alpha}{J(x)} \quad (15)$$

Considering that the viscous time scale

$$t_{\text{visc}} \simeq \frac{r^2}{\nu} \simeq \frac{r}{V_r} \simeq \frac{R_S}{c} x^{3/2} \left(\frac{r}{h}\right)^2 \frac{J(x)}{\alpha} \quad (16)$$

(with  $\nu$  the coefficient of viscosity), the above expression implies  $\nu \simeq r V_r \simeq h V_A [1 + \beta(x)]^{1/2}$ , which if  $V_A$  is replaced by the disk thermal velocity we obtained the standard result of  $\nu \simeq h c_s$ .

Finally, assuming proportionality of the magnetic field with the pressure  $P$  one can employ the equation of hydrostatic equilibrium and the expression of Equation (9), to obtain the scaling of the magnetic field  $B_\phi$ , i.e.,

$$\frac{B_\phi^2}{4\pi} \simeq \frac{n(x) m_p c^2}{2} \frac{1}{x} = \frac{m_p c^2}{\sigma_T R_S} \frac{\dot{m}(x)}{2} x^{-5/2} \left(\frac{r}{h}\right) \frac{J(x)}{\alpha} \quad (17)$$

and from that an expression for the Alfvén velocity; then one can easily see that the scaling of the rate at which magnetic flux is annihilated at the disk plane,  $B_\phi^2 V_A$ , is very similar to that of Equation (10), suggesting that magnetic field annihilation could be the major contributor of accretion disk dissipation.

### 2.3. On ADAF and the Black Hole States

The introduction of Advection-Dominated Accretion Flows [11,12] brought a totally different perspective in accretion flow physics from that of the standard Shakura-Sunyaev [2]. Accretion flows are now allowed to be thick ( $h \simeq r$ ), with their ion temperatures  $T_i \sim m_p (GM/r)^{1/2}$ . The radial force balance is now effected not only by the centrifugal force  $\Omega^2 r$ , but also by the gradient of the radial pressure, and the value of  $\Omega$  is below its Keplerian value  $\Omega_K$ . At the same time, the gas is also heated, in addition to viscous stress heating, also by the radial compression of the flow; this alone leads to a temperature  $T \propto n(x)^{(\gamma-1)}$ , which for adiabatic index  $\gamma = 5/3$  and density  $n(x) \propto x^{-3/2}$ , leads to  $T \propto 1/r$  and combined with viscous heating implies  $\Omega^2 \propto (5\gamma - 3)/r^3 \rightarrow 0$  as  $\gamma \rightarrow 5/3$ , i.e., it precludes rotation of the flow [15]. This issue is circumvented (see [11]) by including the magnetic field contribution to the plasma pressure, which reduces the effective  $\gamma$  below the value 5/3.

As noted in [11], the presence of an ADAF, i.e., a flow with  $h \simeq r$  implies that the plasma remains hot, close to its virial temperature on time scales longer than its accretion time scale. Therefore, demanding its cooling time through Coulomb collisions,  $t_{\text{cool}} \sim 1/n(x)\sigma_T c$  be longer than its viscous (or flow) time scale of Equation (16) implies

$$\frac{R_S}{c} x^{3/2} \left(\frac{r}{h}\right)^2 \frac{J(x)}{\alpha} < \frac{R_S}{c} \frac{1}{\dot{m}(x)} x^{3/2} \left(\frac{h}{r}\right)^3 \frac{\alpha}{J(x)} \quad \text{or} \quad (18)$$

$$\dot{m}(x) < \alpha^2 \quad (19)$$

assuming in the last step that  $h \simeq r$  and  $J(x) \simeq 1$ , i.e.,  $x \gg 3$ . Thus, the presence or not of an ADAF depends on a *single, global* condition on the *normalized* accretion  $\dot{m}$  and it is independent of the flow radius  $x$  or the mass of the system  $M$ . This provides a huge economy of assumptions in interpreting the spectra of accreting black holes, of wide applicability because of the mass independence of this criterion. However, while these flows are mass scale invariant they are of reduced radiative efficiency: Because the viscous time scale is  $\dot{m} (< 1)$  times shorter than the radiative time scale, the power of viscous dissipation, released to heating the protons (same as in the SS73 disks), is advected into the black hole before it can be radiated away; the radiated power then  $\dot{m}$  time smaller than that produced

<sup>1</sup> The electron temperatures are also hot, but their temperature is determined from the balance between Coulomb heating by the much hotter ions and the cooling processes that produce the observed X-ray emission; the cooling of electrons with  $T_e \sim 10^9$  K becomes faster than their heating by protons of any temperature and limits their temperatures at the smallest flow radii to roughly this value.

by viscous dissipation. So for ADAF the expression for the luminosity of Equation (11) should be  $L \propto R_S \dot{m}(x)^2 \propto \dot{m}(x)^2 M$ , rather than  $L \propto \dot{m}(x) M$  that is the case with the standard disks.

The possibility offered by ADAF, namely to include the high energy ( $E > 2$  keV) emission of AGN and XRB as an integral part of the global accretion dynamics, has led to models that combine an SS73 disk at large radii (to produce the quasi-thermal component generally present in the spectra) with a transition of the flow to an ADAF at a radius  $r < r_{tr}$  that accounts for their high energy X-rays. This way, one could reproduce the entire spectrum with a single accretion flow [13]. To account for the increasing dominance of the quasi-thermal disk component with the source luminosity, observed in individual XRBs on increase of their bolometric luminosity and in AGN statistically (by the variation of their  $\alpha_{OX}$  index with luminosity [4]), they proposed that the transition radius,  $r_{tr}$ , decreases with increasing luminosity. While appealing at first sight, these models vitiate the ADAF dependence of the single global  $\dot{m}$ . It is also hard to see how a cool, thin outer disk will convert into an ADAF at  $r < r_{tr}$ ; finally, it is also not obvious why  $r_{tr}$  would decrease with source luminosity. Some of these issues will be discussed in Section 4 with consideration of radius dependent accretion rates.

### 3. Accretion Disks Winds: An AGN Rosetta Stone?

The launch of HST, Chandra and XMM-Newton, ushered a new era in the study of accreting black holes and especially AGN. These observatories discovered that  $\simeq 50\%$  of AGN exhibit blue-shifted absorption features in the UV and X-ray spectra [14], presumably a manifestation of the presence of winds that are ubiquitous in accreting black holes. Of particular interest are the absorption features of their X-ray spectra, because they span a large range in velocity ( $v \sim 0.5 c$  to  $v \simeq 300\text{--}500$  km/s) and in ionization states of the plasma (from Fe XXVI to Fe II, much larger than their UV counterparts; the power of X-ray spectroscopy lies in that in the span of 1.5 decades in energy it encompasses ions that span 5 decades in ionization parameter  $\zeta$ ). These absorption features are thought to be the result of a wind photoionized by the AGN continuum and are broadly referred to as Warm Absorbers (WA), because of the inferred temperature of the corresponding plasma.

#### 3.1. X-Ray Absorbers: Their Phenomenology and Implications

Considering that the observed winds are photoionized by the radiation of a point-like X-ray source and that we observe the radiation along a pencil beam from the X-ray source to us, the absorption spectra should probe the continuum of velocities,  $v(r)$ , columns,  $N_H(r)$ , and densities,  $n(r)$ , of the outflowing plasmas and the continuum of ionization parameter  $\zeta = L/n(r)r^2 = L/N_H(r)r$  along the observer's line of sight (LoS). Therefore, measurement of the absorption depth i.e., equivalent width (EW), (and also the velocity width if possible) of a transition, known to exist at a given range in  $\zeta$ , provides the local wind column,  $N_H$  (and velocity), while its  $\zeta$ -value (for the observed  $N_H$  and  $L$ ) provides a measure of the distance of the given ion from the ionizing source, along the observer's LoS. Observations of  $N_H, \zeta$  for multiple ions can then be inverted to probe the wind density (and velocity) structure along our LoS.

This was in essence the approach of Behar and collaborators, ([21], hereafter HBK07) and ([22] hereafter B09). In these two important papers, HBK07 and B09 introduced what they called the Absorption Measure Distribution  $AMD \equiv dN_H/d \log \zeta$ , namely the Hydrogen equivalent column of an ion,  $N_H$ , per  $\log \zeta$ . Assuming a power-law functional dependence of  $N_H$  on  $\zeta$ , namely  $N_H \propto \zeta^\alpha$ , they produced a global fit of the detected, distinct ionic species of as many different elements as the observations allowed, to obtain a value for  $\alpha$ . (Figure 1(Left)). It is important to note that for a spatially smooth outflow, this relation implies a power-law density dependence on the wind along the observer's LoS, i.e.,  $n(r) \propto r^{-s}$ , with  $s$  and  $\alpha$  related via  $s = (2\alpha + 1)/(\alpha + 1)$ . The values of  $\alpha$  were found to be  $\alpha \simeq 0 - 0.3$ , implying  $s \simeq 1 - 1.24$  and  $N_H \propto r^{-s+1} \propto r^0 - r^{0.24}$ , a very weak  $r$ -dependence.

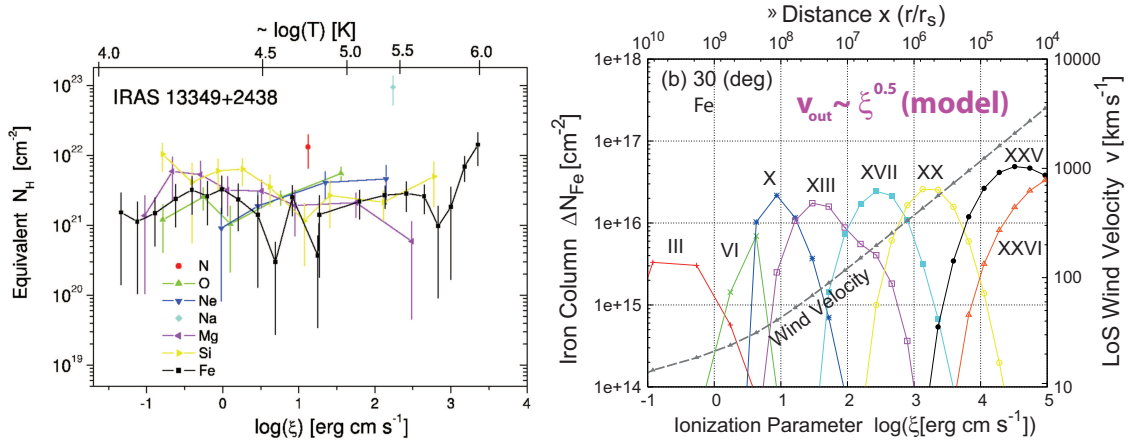


**Figure 1.** (Left) The AMD of IRAS 13349+2438 (from [21]) determined independently from the transitions of each element and ionization state shown. The weak dependence of  $N_H$  on  $\xi$  is apparent. (Right) The ionization structure of Fe for a model with  $s = 1$  and  $\theta = 30$  deg. The ionization state of Fe decreases with increasing distance; however, the maximum  $N_H$  of each ion remains roughly constant (from [17]). Also shown is the wind velocity with distance, indicating that lower ionization ions have lower velocities.

The broad range in  $\xi$  ( $\sim 5$  decades) and the almost ‘flat’  $N_H - \xi$  relation observed, preclude that the WA outflows be driven by radiation pressure or X-ray heating; such winds, because they are launched from regions of limited size,  $R_l$ , they produce, at distances a few ( $\sim 10$ ) times  $R_l$  constant mass flux and velocity, resulting in density  $n(r) \propto 1/r^2$  and  $N_H \propto r^{-1}$ , in gross disagreement with observation; in their accelerating phase, their density dependence is a steeper function of  $r$   $n(r) \propto r^{-3}$ , implying that their  $\xi$  should decrease with  $r$  and so should their velocity,  $v(r)$ , while their column should be larger at smaller  $r$ . All these dependencies disagree with observation.

To interpret the AMD relation and the WA observations of HBK07 and B09, Fukumura, Kazanas and collaborators [17,18] (FKCB10a,b) concluded that these winds must be two dimensional (2D), launched across the entire disk domain. Motivated by these considerations they computed the photoionization of the self-similar 2D MHD winds of Contopoulos & Lovelace ([23] hereafter CL94). These are 2D winds, generalizations of those of Blandford & Payne [24]. Because of their broad radial extent, they offer the possibility of a wide range of  $\xi$ ; indeed the winds of CL94 provide radial density profiles of the form  $n(r) \sim r^{-s}$  ( $s \simeq 1$ ),  $v(r) \propto r^{-1/2}$ , consistent with the values inferred from the AMD analysis.

The winds of [24] imply radial density profiles  $n(r) \propto r^{-3/2}$  which are too steep to be consistent with the WA data; however, the broad range of their launching radii has prompted several authors [25,26] to employ them in modeling the AGN UV and optical line profiles.

### 3.2. The Wind Scaling Relations

The results of FKCB10a, though motivated by specific AGN, are quite general: The MHD Accretion disk winds, whose local velocities scale with the Keplerian (see CL94), are self-similar if the radius  $r$  is normalized to the BH Schwarzschild radius  $R_S$  ( $x = r/R_S$ ,  $R_S = 3 \mathcal{M}$  km, with  $\mathcal{M} \equiv (M/M_\odot)$ ), their velocity to  $c$  ( $v(x)/c = x^{-1/2}$ ) and the mass flux rate  $\dot{M}$  to the Eddington rate, i.e.,  $\dot{m} = \dot{M}/\dot{M}_E$ ,  $\dot{M}_E \equiv L_E/c^2$  ( $L_E \simeq 1.3 \times 10^{38} \mathcal{M}$  erg s<sup>-1</sup> is the Eddington luminosity). So mass conservation in physical and dimensionless units reads respectively

$$\dot{M}(r, \theta) \sim n(r, \theta) r^2 v(r) \quad \text{or} \quad \dot{m}(x) \mathcal{M} \propto n(x) \mathcal{N}(\theta) x^2 \mathcal{M}^2 x^{-1/2}. \quad (20)$$

with  $\mathcal{N}(\theta) \simeq e^{5(\pi/2 - \theta)}$  (see Figure 2(Left) of FKCB10a). The density normalization is such that (integrated over  $\theta$ )  $n(x \simeq 1) \sigma_T R_S \simeq \tau(x \simeq 1) \sim 3 \cdot 10^5 \mathcal{M} \sigma_T n(1) \simeq \dot{m}_0$ , with  $\dot{m}_0$  the (normalized) mass

flux at the smallest wind radius ( $x \gtrsim 1$ ). For a density profile such as that obtained from fits to the AGN WA, namely for  $n(x) \propto x^{-s}$  we obtain,

$$\dot{m}(x) \simeq \dot{m}_0 x^{-s+3/2} \quad \text{and} \quad N_H(x) \propto \mathcal{N}(\theta) \dot{m}_0 x^{-s+1} \quad (21)$$

The relations of Equation (21) then suggest that for  $s \simeq 1$  the wind mass flux increases with radius like  $x^{1/2}$ , while the column is roughly constant independent of the distance, in agreement with the properties of ADIOS [15].

The wind ionization parameter  $\zeta$ , can also be cast in dimensionless units: If  $\eta$ , ( $\simeq 10\%$ ) is the radiative efficiency of the accretion process, then the luminosity  $L$  can be written as  $L \simeq 10^{38} \eta \dot{m}_a \mathcal{M}$  erg/s ( $\dot{m}_a$  is the dimensionless accretion rate onto the BH to produce the luminosity  $L$ ), yielding the for  $\zeta$

$$\zeta(x) \simeq \frac{L}{n(r)r^2} \simeq \frac{\eta \dot{m}_a}{N_H(x)x} \simeq 10^8 \frac{\eta}{f_w \mathcal{N}(\theta)} \frac{\mathcal{S}(v_{\text{ion}})}{x^{-s+2}} \text{ erg cm s}^{-1} \quad (22)$$

where  $f_w = \dot{m}_0/\dot{m}_a$  ( $\sim 1$ ) is the ratio of mass flux in wind and in accretion at the smallest radii and  $\mathcal{S}(v_{\text{ion}})$  is a factor that determines the ionizing fraction of the bolometric luminosity produced by accretion onto the BH, related to the AGN  $\alpha_{\text{OX}}$ .

With respect to Equations (21) and (22), that provide the expression for the winds' mass flux, column and ionization, one should note that: (a) They are independent of the BH mass  $\mathcal{M}$  and as such they could apply to an accreting black hole of any mass [27]. (b) The wind column  $N_H$  depends mainly on the dimensionless mass flux at the smallest radii  $\dot{m}_0$  and, depending on the value of  $s$ , it has a weak dependence on the (dimensionless) distance from the black hole  $x$ ; however, it has a very strong dependence on the observer inclination angle  $\theta$  giving the wind the toroidal appearance implied by the AGN unification scheme. (c) The wind ionization parameter  $\zeta$  is independent of both  $\dot{m}$  and  $\mathcal{M}$  and depends only on the (dimensionless) distance from the black hole  $x$  and the observer inclination angle  $\theta$ . However, the wind's ionization structure and appearance (i.e., the velocities of its absorption features and the angular dependence of their column) depend crucially on the fraction of ionizing photons in the spectrum  $\mathcal{S}(v_{\text{ion}})$  ( $\alpha_{\text{OX}}$  serves as its proxy in AGN) [18] and  $\mathcal{N}(\theta)$ .

Our basic premise is that these winds are launched across the entire disk extent with velocities  $v(x) \propto x^{-1/2}$ , in all accreting BH; as a result, the scalings discussed above should also correlate with the velocities of observed absorption features. In AGN with high X-ray content (Seyferts) the wind's inner region is fully ionized out to  $x \gtrsim 10^3$ , resulting in the occurrence of the highest  $\zeta$  ( $\sim 10^4, 10^5$ ) absorption transitions (Fe XXV, Fe XXVI) at  $v \sim cx^{-1/2} \sim 10,000$  km/s; in the lower X-ray content BAL QSOs, the fully ionized region is much smaller ( $x \sim 10 - 30$ ) and the corresponding velocities much higher ( $v \sim 0.3c$ ; APM 08279+5255) [18,28]; finally, in galactic XRBs with  $\mathcal{S}(v_{\text{ion}}) \simeq 1$  the wind is ionized out to  $x \gtrsim 10^5$  and the absorber velocities are  $v \sim 300 - 1000$  km/s [27], in agreement with our scalings.

We have discussed in this section the mass scale invariance of the MHD winds and the dependence of their obscuration (i.e.,  $N_H(x, \theta)$ ,  $\zeta(x, \theta)$ ) and their absorber velocities on sources' content of ionizing radiation and the wind mass flux. To close the gap in AGN (or XRB) phenomenology, one is left with finding a relation between the AGN (dimensionless) accretion rate  $\dot{m}$  and the X-ray content, or broadly, the relative strengths of the BBB and the X-ray emission. This is discussed in the next section.

#### 4. Accretion Disk Spectral Energy Distributions (SEDs)

It was shown above that the disk wind density profiles implied by the X-ray absorber observations are of the form  $n(x) \propto x^{-s}$ , with  $s \simeq 1$ . However (see Equation (21)), for winds with  $s < 3/2$  the wind mass flux increases with radius, implying that the disk accretion rate must decrease toward the BH! ; as a result, only a small fraction of the available mass accretes onto the black hole [15]. Most importantly, if below some radius,  $x_{tr}$ , the local accretion disk rate drops below the critical rate  $\dot{m} \simeq \alpha^2$  ( $\alpha$  is the disk viscosity parameter), then (see Equation (19)) the disk can potentially make a transition to an

ADAF flow [11], in fact an ADIOS; this hot ( $T \simeq 10^9$  K) segment occupies the AGN innermost region and constitutes the site of X-ray emission, in agreement with the X-ray variability properties and the microlensing observations.

However, the condition of Equation (19) for the presence of an ADAF is necessary but not sufficient. One must still address the issue of heating up the "cold" protons of the outer part of the disk to their virial value, at  $r < r_{tr}$ . In the absence of a more detailed theory, we propose here that their heating takes place at the equatorial current sheet of the accretion disk. The current sheet dissipation can provide energies for protons (and electrons) close to their virial one; the ability to retain these energies sufficiently long to affect the disk structure depends on the disk average density at this specific radius, i.e., on the local value of  $\dot{m}$ . Therefore, the picture of black hole states envisioned in [13] can be realized for accretion disks with variable (in  $r$ ) accretion rates.

In Figure 2(Middle,Right) below we show the SEDs of two AGN: the Broad Line Seyfert 1 (BLS1) galaxy NGC 5548 [29] and that of the Narrow-Line Seyfert 1 (NLS1) PG 1244+026 [30]. These exemplify the drastically different SED distributions of these two Seyfert galaxies, even though they both belong to the same broad AGN category. Their most obvious difference is that of the relative importance of their BBB (Optical-UV) and X-ray emissions. The bolometric luminosity of NGC 5548 is dominated by the X-ray emission, while that of the PG 1244+026 by the UV one. Considering that it is broadly assumed that the BBB emission comes from a disk that terminates in the ISCO, one would expect that emission to be always the dominant one.

We propose that this distinctive difference is related to the radius-dependent mass accretion rate of their corresponding disks, effected by the presence of MHD winds which remove progressively most of the mass available for accretion as the disk plasma sinks toward the black hole. As we noted earlier when, at some transition radius  $r_{tr}$ , the local accretion rate becomes smaller than  $\alpha^2$ , the disk transits to an ADAF (or rather an ADIOS) state for radii  $r < r_{tr}$ , while maintaining the standard SS73 disk form at  $r > r_{tr}$ . Considering that at its  $r < r_{tr}$  segment, where the X-rays are produced, the luminosity has smaller efficiency with  $\dot{m}$ , i.e.,  $L_X \propto \dot{m}(r)^2$  vs.  $L_{UV} \propto \dot{m}(r)$  for  $r > r_{tr}$ , but it is produced at a deeper gravitational potential, their relative ratios will depend on the transition radius  $r_{tr}$ . Furthermore, as the global mass flux, i.e., that provided at the outer edge of the accretion flow,  $\dot{m}(x)$ , and the ensuing luminosity increase, the transition radius  $r_{tr}$  will shift to smaller  $r$ , with the importance of the thermal component increasing, as suggested by [13] in their attempt to account for the XRB spectral evolution.

With the above qualifications and assumptions, we can express quantitatively the relative importance of the BBB and X-ray components in the AGN spectra. We assume, to be specific, that the index  $s \simeq 1$ , so that  $x_{tr}$  is given by the expression

$$\dot{m}(x_{tr}) = \dot{m}_0 x_{tr}^{1/2} \simeq \alpha^2 \quad (23)$$

Then from Equation (11) we obtain the following expressions of  $L(x > x_{tr})$  and  $L(x < x_{tr})$

$$L(x > x_{tr}) \propto \int_{x_{tr}}^{\infty} \frac{\dot{m}(x)}{x} J(x) d \ln x \sim \frac{\dot{m}_0}{x_{tr}^{1/2}} \left[ 1 - \frac{\zeta}{2} \left( \frac{x_I}{x_{tr}} \right)^{1/2} \right] \quad (24)$$

$$L(x < x_{tr}) \propto \int_{x_I}^{x_{tr}} \frac{\dot{m}(x)^2}{x} J(x) d \ln x \sim \dot{m}_0^2 \left[ \ln \left( \frac{x_{tr}}{x_I} \right) - 2\zeta + 2\zeta \left( \frac{x_I}{x_{tr}} \right)^{1/2} \right] \quad (25)$$

One should note that the ratio  $R$  of these two luminosities is proportional to  $1/\alpha^2$ :

$$R = \frac{L(x > x_{tr})}{L(x < x_{tr})} = \frac{1}{\dot{m}_0 x_{tr}^{1/2}} \left( \frac{P1}{P2} \right) = \frac{1}{\alpha^2} \left( \frac{P1}{P2} \right) \quad (26)$$

with the last equality because of Equation (23) and with  $P1$ ,  $P2$  the values of the square brackets in Equations (24) and (25) respectively.

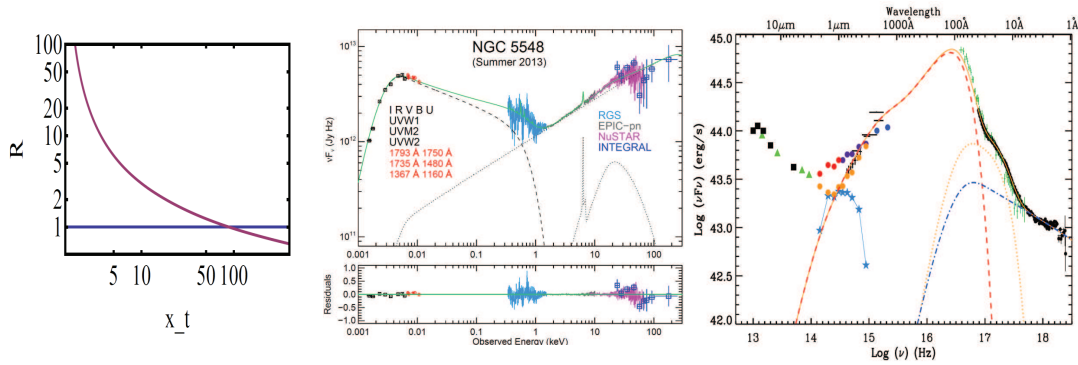


**Figure 2.** (Left) The ratio  $R$  of the thermal (BBB) to the X-ray bolometric luminosities as a function of the transition radius  $x_t$  from the SS73 to the ADAF disk regime. (Middle) The  $\nu F_\nu$  spectrum of NGC 5548 (from [29]) indicating a slight dominance of the X-ray luminosity, implying for this case that  $x_t \gtrsim 100$ . (Right) Same as (Middle) but for the NLS1 PG 1124+026 (from [30]); in this case the BBB component is dominant implying  $x_t \lesssim 5$ .

Figure 2(Left) depicts the ratio  $R$  as a function of the transition radius  $x_{tr}$ , for  $x_I = 1.5$ ,  $\zeta = 1$  and  $\alpha = 1/3$ .<sup>2</sup> Of interest in this figure is the value of  $x_{tr} \simeq 100$  for which  $R \simeq 1$ , because this sets the size of the disk at which the cool/thin disk quasi-thermal luminosity matches that of the harder radiation produced in the advection-dominated accretion flow section. This will then correspond to the spectrum of NGC 5548 of Figure 2(Middle). On the other hand, the spectrum of PG 1124+026, implies  $x_{tr} \simeq 3 - 5$ , consistent with the larger  $\dot{m}$  associated with NLS1 galaxies. The spectra are also steeper, considering that the transfer of proton energy to electrons is not very efficient in the narrow range of radii that the ADAF flow is allowed in this AGN.

## 5. Discussion, Conclusions

We described above that the multidimensional phenomenology associated with the appearance and spectral distribution of AGN (and XRB) can be reduced to a small number of dimensionless global parameters of these systems, most notably the dimensionless accretion rate  $\dot{m}$  and their disk inclination angle  $\theta$ . The underlying black hole mass, while important in providing a scale of the absolute luminosity for a given  $\dot{m}$ , it is also important in determining the temperature of the thermal BBB component of the accretion disk; however, this effect is only weakly dependent on this mass ( $\propto M^{-1/4}$ ), it is well understood and largely under control. Apart from this component, the rest of the accretion disk and wind properties (ionization, column density, velocity) appear to be mass independent. While many details remain elusive, the radial dependence of the disk accretion rate, implied by the apparent increase in the wind mass flux with radius, is the crucial novel notion in this analysis. It is this notion that allows for a coherent picture of their combined X-ray–UV–Optical spectra, with the relative importance and spatial location of these components strongly dependent on the value of  $\dot{m}$  as described and in good agreement with observation. Finally, the angular dependence of the MHD winds, implies a strong dependence of their properties on the disk inclination angle, a feature generally known as AGN Unification. While some reasons for the inferred increase in the disk wind mass flux with distance are given above, the detailed underlying physics of this most important issue, namely the connection the disk structure with the wind properties is still not entirely clear. We hope that this note will motivate a more focused activity on this issue. Perhaps the generation of magnetic flux near the disk inner edge by the Cosmic Battery effect [32–34] plays a role in this respect.

<sup>2</sup> While this value may appear too large, one should note that [20], argue that for disks at which the pressure is dominated by magnetic fields  $\alpha = 1/\sqrt{3}$ , while [31] in their study of shear-box simulations with a net magnetic flux find  $\alpha \simeq 1$  for disks with gas to (poloidal) magnetic pressure, greater than 0.01.

We have refrained in this note from discussing the line emission in AGN. This constitutes an entire subject onto itself. We believe that it is relevant to the issues discussed herein because the plasma responsible for the absorption will also produce line emission. Actually, the X-ray absorbers that motivated our work probe only a small fraction of the entire wind phase space, namely the small pencil beam from the X-ray source along the observer's LoS; the AGN line emission provides information about the entire phase space of these winds; it remains to be seen whether it is consistent with the ideas promoted herein. There is clearly more work to be done; we believe that our work points to the correct direction.

Finally, the issue of MHD winds discussed in the previous sections, while focused on radio quiet AGN, is also relevant to the physics of radio loud ones, in particular blazars. The reason for that is that these winds, of columns that depend mainly on  $\dot{m}$ , reprocess and isotropize the disk radiation so that it can be reprocessed by the relativistic jet propagating along the disk axis as "External Inverse Compton"  $\gamma$ -rays. In a recent publication [35] we showed how the blazar phenomenology, known as the "blazar sequence" can be reproduced by variation of a single parameter, that again being  $\dot{m}$ , indicating an underlying economy of parameters across the entire field of AGN physics.

**Funding:** This research received no external funding.

**Acknowledgments:** The author would like to acknowledge financial support by NASA's ADAP program and GI grants from Chandra and Fermi. He would also like to acknowledge numerous discussions and interactions with his collaborators, K. Fukumura, E. Behar, I. Contopoulos, C. Shrader and F. Tombesi.

**Conflicts of Interest:** The authors declare no conflict of interest.

## References

1. Abramowicz, M.A.; Fragile, P.C. Foundations of Black Hole Accretion Disk Theory. *Living Rev. Relativ.* **2013**, *16*, 1–88. [[CrossRef](#)] [[PubMed](#)]
2. Shakura, N.; Sunyaev, R. Black Holes in Binary Systems. Observational Appearance. *Astron. Astrophys.* **1973**, *24*, 337–355.
3. Galeev, A.A.; Rosner, R.; Vaiana, G.S. Structured Coronae of Accretion Disks. *Astrophys. J.* **1979**, *229*, 318–326. [[CrossRef](#)]
4. Steffen, A.T.; Strateva, I.; Brandt, W.N.; Alexander, D.M.; Koekemoer, A.M.; Lehmer, B.D.; Schneider, D.P.; Vignali, C. The X-Ray-to-Optical Properties of Optically Selected AGN over Wide Luminosity and Redshift Ranges. *Astron. J.* **2006**, *131*, 2826–2842. [[CrossRef](#)]
5. Done, C.; Gierlinski, M.; Kubota, A. Modelling the Behaviour of Accretion Flows in X-ray Binaries. *Astron. Astrophys. Rev.* **2007**, *15*, 1–66. [[CrossRef](#)]
6. Haardt, F.; Maraschi, L. X-Ray Spectra from Two-Phase Accretion Disks. *Astrophys. J.* **1993**, *413*, 507–517. [[CrossRef](#)]
7. Berkeley, A.J.; Kazanas, D.; Ozik, J. Modeling the X-Ray-Ultraviolet Correlations in NGC 7469. *Astrophys. J.* **2000**, *535*, 712–720. [[CrossRef](#)]
8. Balbus, S.; Hawley, J. A Powerful Local Shear Instability in Weakly Magnetized Disks. *Astrophys. J.* **1991**, *376*, 214–233. [[CrossRef](#)]
9. Christodoulou, D.; Contopoulos, I.; Kazanas, D. Interchange Method in Incompressible Magnetized Couette Flow: Structural and Magnetorotational Instabilities. *Astrophys. J.* **1996**, *462*, 865–873. [[CrossRef](#)]
10. Christodoulou, D.; Contopoulos, I.; Kazanas, D. Interchange Method in Compressible Magnetized Couette Flow: Magnetorotational and Magnetoconvective Instabilities. *Astrophys. J.* **2003**, *462*, 373–383. [[CrossRef](#)]
11. Narayan, R.; Yi, I. Advection-dominated accretion: A self-similar solution. *Astrophys. J.* **1994**, *428*, L13–L16. [[CrossRef](#)]
12. Narayan, R.; Yi, I. Advection-dominated accretion: Self-similarity and bipolar outflows. *Astrophys. J.* **1995**, *444*, 231–243. [[CrossRef](#)]
13. Esin, A.A.; McClintock, J.E.; Narayan, R. Advection-Dominated Accretion and the Spectral States of Black Hole X-Ray Binaries: Application to Nova Muscae 1991. *Astrophys. J.* **1997**, *489*, 865–889. [[CrossRef](#)]

14. Crenshaw, D.M.; Kraemer, S.B.; George, I.M. Mass Loss from the Nuclei of Active Galaxies. *Ann. Rev. Astron. Astrophys.* **2003**, *41*, 117–167. [[CrossRef](#)]
15. Blandford, R.D.; Begelman, M.C. On the Fate of Gas Accreting at a Low Rate on to a Black Hole. *Mon. Not. R. Astron. Soc.* **1999**, *211*, P1–P5. [[CrossRef](#)]
16. Novikov, I.D.; Thorn, K.S. Astrophysical Black Holes. In *Black Holes*; by DeWitt, C., DeWitt, B.S.; Eds.; Gordon and Breach: New York, NY, USA, 1972; pp. 343–450.
17. Fukumura, K.; Kazanas, D.; Contopoulos, I. Behar, E. MHD Accretion Disk Winds as X-ray Absorbers in Active Galactic Nuclei. *Astrophys. J.* **2010**, *715*, 636–650. [[CrossRef](#)]
18. Fukumura, K.; Kazanas, D.; Contopoulos, I. Behar, E. Modeling High-velocity QSO Absorbers with Photoionized MHD Disk Winds. *Astrophys. J.* **2010**, *723*, L228–L232. [[CrossRef](#)]
19. Svensson, R.; Zdziarski, A.A. Black Hole Accretion Disks with Coronae. *Astrophys. J.* **1994**, *436*, 599–606. [[CrossRef](#)]
20. Pariev, V.I.; Blackman, E.G.; Boldyrev, S.A. Extending the Shakura-Sunyaev Approach to a Strongly Magnetized Accretion Disk Model. *Astron. Astrophys.* **2003**, *407*, 403–421. [[CrossRef](#)]
21. Holczer, T.; Behar, E.; Kaspi, S. Absorption Measure Distribution of the Outflow in IRAS 13349+2438: Direct Observation of Thermal Instability? *Astrophys. J.* **2007**, *663*, 799–807. [[CrossRef](#)]
22. Behar, E. Density Profiles in Seyfert Outflows. *Astrophys. J.* **2009**, *703*, 1346–1351. [[CrossRef](#)]
23. Contopoulos, J.; Lovelace, R.V.E. Magnetically driven jets and winds: Exact solutions. *Astrophys. J.* **1994**, *429*, 139–152. [[CrossRef](#)]
24. Blandford, R.D.; Payne, D.G. Hydromagnetic flows from accretion discs and the production of radio jets. *Mon. Not. R. Astron. Soc.* **1982**, *199*, 883–903. [[CrossRef](#)]
25. Emmering, R.T.; Blandford, R.D.; Shlosman, I. Magnetic acceleration of broad emission-line clouds in active galactic nuclei. *Astrophys. J.* **1992**, *385*, 460–477. [[CrossRef](#)]
26. Bottorff, M.C.; Korista, K.T. Shlosman, I.; Blandford, R.D. Dynamics of Broad Emission-Line Region in NGC 5548: Hydromagnetic Wind Model versus Observations. *Astrophys. J.* **1997**, *479*, 200–221. [[CrossRef](#)]
27. Fukumura, K.; Kazanas, D.; Shrader, C. R.; Tombesi, F.; Behar, E.; Contopoulos, I. Magnetic origin of black hole winds across the mass scale. *Nat. Astron.* **2017**, *1*, 62–72. [[CrossRef](#)]
28. Chartas, G.; Brandt, W.N.; Gallagher, S.C.; Garmire, G.P. Chandra Detects Relativistic Broad Absorption Lines from APM 08279+5255. *Astrophys. J.* **2002**, *579*, 169–175 [[CrossRef](#)]
29. Mehdipour, M.; Kaastra, J.S. Anatomy of the AGN in NGC 5548: I. A global model for the broadband spectral energy distribution. *Astron. Astrophys.* **2015**, *575*, A22–A39. [[CrossRef](#)]
30. Jin, C.; Done, C.; Middleton, M.; Ward, M. A long XMM-Newton observation of an extreme narrow-line Seyfert 1: PG 1244+026. *Mon. Not. R. Astron. Soc.* **2013**, *436*, 3173–3185. [[CrossRef](#)]
31. Bai, X.-N.; Stone, J.M. Local Study of Accretion Disks with a Strong Vertical Magnetic Field: Magnetorotational Instability and Disk Outflow. *Astrophys. J.* **2013**, *767*, 30–48. [[CrossRef](#)]
32. Contopoulos, I.; Kazanas, D. A Cosmic Battery. *Astrophys. J.* **1999**, *508*, 859–863. [[CrossRef](#)]
33. Contopoulos, I.; Kazanas, D.; Christodoulou, D. M.: The Cosmic Battery Revisited. *Astrophys. J.* **2006**, *652*, 1451–1456. [[CrossRef](#)]
34. Christodoulou, D.M.; Contopoulos, I.; Kazanas, D. Simulations of the Poynting–Robertson Cosmic Battery in Resistive Accretion Disks. *Astrophys. J.* **2008**, *674*, 388–407. [[CrossRef](#)]
35. Boula, S.; Kazanas, D.; Mastichiadis, A. Accretion Disk MHD Winds and Blazar Classification. *Mon. Not. R. Astron. Soc.* **2019**, *482*, L80–L84. [[CrossRef](#)]

